

MRS, μ EDXRF and FTIR-ATR analysis of white paste inlays in Bronze Age pottery from the southeast of the Iberian Peninsula: the case of Peñalosa (Jaén, Spain)

Laura Vico Triguero^{a*1}, José Alfonso Tuñón López^b, Alberto Sánchez Vizcaíno^b, Jesús Gámiz Caro^a, Marta Moreno García^c, Francisco Contreras Cortés^a

^a Departamento de Prehistoria y Arqueología, Universidad de Granada, Campus Universitario de Cartuja s/n, 18071 Granada, España.

^b Instituto Universitario de Investigación en Arqueología Ibérica, Universidad de Jaén, Campus Las Lagunillas s/n 23071, Edif. C6, Jaén, España.

^c Instituto de Historia, CSIC, Albasanz 26-28, 28037 Madrid, España.

Abstract

The objective of this paper is to characterise the composition and manufacturing techniques of the white paste fillings in the Bronze Age pottery decorations on the eastern Iberian Peninsula, using as a case study the Argaric archaeological site of Peñalosa (Baños de la Encina, Jaén). The determination of the characteristics and manufacture of these pastes required the application of analytical techniques such as micro-Raman spectroscopy (MRS), micro X-ray fluorescence (μ EDXRF) and Fourier transform infrared spectroscopy (FTIR-ATR), as well as reference materials. This methodology made it possible to distinguish two types of production in this enclave: one with bone and the other with kaolinite. The coexistence of different manufacturing techniques had already been corroborated in other Bronze Age contexts in Europe and the southwest of the Iberian Peninsula. We were also able to determine that, in the case of paste made with bone, the temperatures would have reached 800°C, making it possible to link the use of calcined deer antlers with the manufacture of these decorations.

Keywords: White paste inlay, deer antler, spectroscopic analysis, Bronze Age, Iberian Peninsula

1. Introduction

The study of the white paste decoration on prehistoric pottery is an area of research that has generated considerable interest. This is because both its composition and its production technology have proven to be synonymous with the cultural identity of certain peoples or regions throughout prehistory, as well as with technological changes fostered by the arrival of new peoples, ideas or materials (Odriozola 2018). The most highly developed archaeometric studies of decorative white-paste fillings in Europe are those carried out in Hungary, where its use from the Neolithic to the Bronze Age has been documented using analytical techniques such as XRD, SEM, FTIR, LA-ICP-MS and μ PIXE (Gherdán et al. 2003; Sziki et al. 2003; Roberts et al. 2008; Parkinson et al. 2010; Sofaer and Roberts 2016). Also noteworthy are other studies of white pastes that cover the same periods in the Piedmont region (northern Italy) where IR-spectroscopy

¹ Corresponding author: Laura Vico Triguero
e-mail address: lvico@ugr.es

and XRD have been used (Giustetto et al. 2013) and in Scotland using SEM-EDX, μ XRF, XRD and FTIR (Jones et al. 2015). In Moravia (Czech Republic) research has focused on the Late Bronze and Copper Ages using XRD (Všianský et al. 2014) and in Bulgaria on the Early and Late Chalcolithic using FTIR, LIBS and XRD (Pirovska et al. 2020). More closely focused on the Neolithic, of particular note is the work carried out in Serbia, where FTIR and XRF were applied (Perišić et al. 2016), in Croatia using SEM-EDS and XRD (Kos et al. 2015), and in Poland where thin section petrography was used (Zastawny et al. 2012).

Compared to the aforementioned cases, on the Iberian Peninsula there have been very few archaeometric studies that have looked in depth at the techniques and type of materials used to manufacture these white pastes and they have been very limited in scope, especially with regard to the Bronze Age. The main research has focused on the west of the Iberian Peninsula (southern Portugal, Galicia, Extremadura, Castile and León and the western part of Andalusia) and has been carried out on the white paste fillings of Chalcolithic bell beaker pottery (Odriozola y Hurtado 2007; Odriozola y Martínez 2007; Odriozola et al. 2012; Odriozola 2018; Lantes-Suárez et al. 2010). With regard to Bronze Age white-filled pottery, specifically those designated Proto-Cogotas and Cogotas I on which this paper focuses, archaeological studies are even more scarce. Only some sherds from the northern Meseta and Extremadura have been analysed using FTIR-ATR and XRD (Odriozola et al., 2012; Martín-Gil and Martín-Gil 2009), although these white paste fillings are attested in other areas of the Iberian Peninsula, such as the southeast.

Within the framework of the Argaric culture –the most representative of the Iberian Peninsula Bronze Age cultures, located in the southeast– a small amount of pottery with decorations filled with white paste has been found. One of the archaeological sites that offers this type of well-contextualised and well-dated decoration is Peñalosa. This settlement, whose occupation is attributed to the Argaric Full Bronze Age (1850-1450 BC) (Contreras et al. 2014), in the Alto Guadalquivir region in the municipality of Baños de la Encina (Jaén, Spain) (Figure 1). Five proto-Cogotas sherds with part of their white paste fillings preserved have been recovered at this site. The archaeometric analysis of these pastes and their manufacturing technology is a pioneering study in the field of the Argaric culture in particular and of the Iberian Peninsula Bronze Age in general.

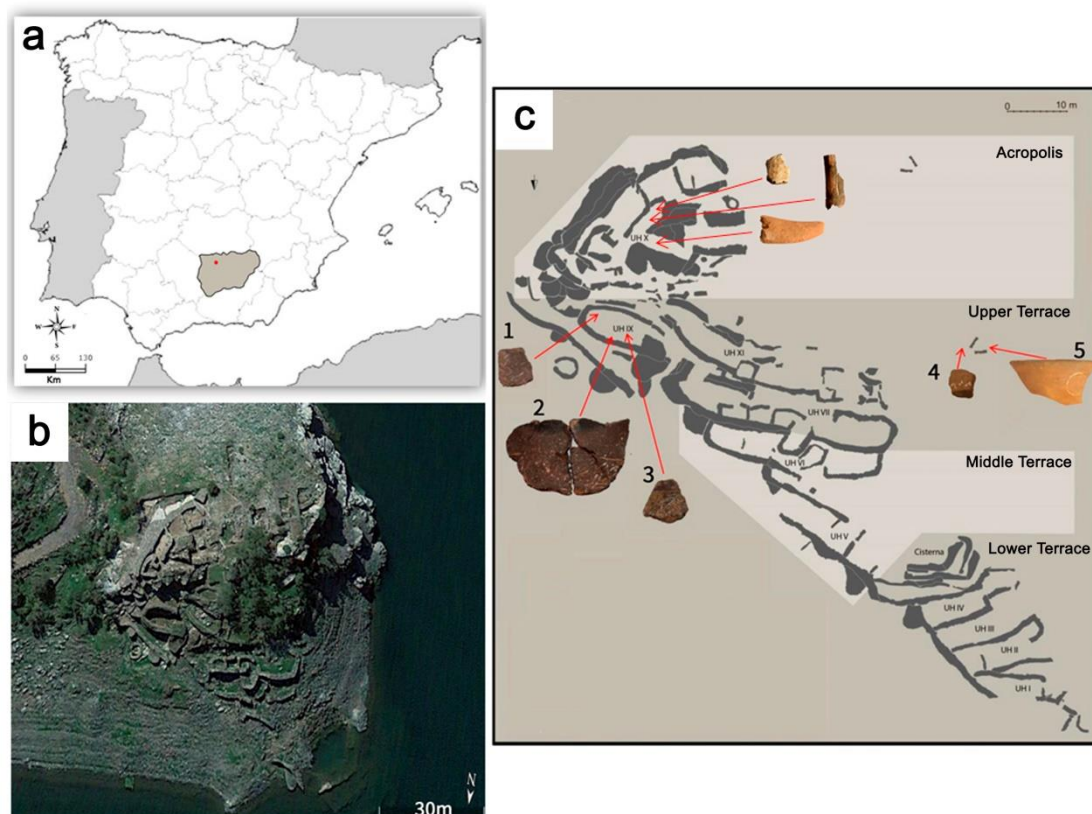


Figure 1. a) Location of the Peñalosa archaeological site (Baños de la Encina, Jaén, Spain). b) Aerial view of the site. c) Contextualisation of the pottery fragments and antlers analysed in the general plan of the Peñalosa settlement (reworked from García-García, 2018).

Nevertheless, the presence of this type of decoration in Argaric contexts has been the subject of debate, as it is more frequent in the Meseta area (Abarquero 2005). The case of Peñalosa is even more controversial due to the very early chronologies of the pottery analysed, which place them around 1700 BC (Contreras, 2000; Contreras and Alarcón, 2012). Therefore, the identification of possible areas of influence based on the technology used to manufacture these pastes is essential for us to understand their presence in this area. In this respect, Peñalosa plays a very important role, since its strategic location associated with metal extraction and manufacture (Contreras et al. 2014) places it on the border between the southeast of the Iberian Peninsula and the Meseta (central plateau). Therefore, the study of its artifacts can serve as a starting point for defining possible interregional contacts.

Given all these factors, this paper has the following objectives:

- To determine the physical-chemical composition of the white paste incrustations of the Peñalosa pottery in order to ascertain the type of material used in their manufacture in the Alto Guadalquivir area.
- To obtain information on the technical process used to make these pastes, as well as the degree of specialisation in their manufacture based on the selection of certain raw materials and the complexity of their production. The starting hypothesis is the use of deer antlers.
- To obtain a broader perspective on the possible connections between the territories and peoples of the Iberian Peninsula, as well as the evolution of technological traditions from previous periods.

To achieve these objectives, a multi-analytical method was applied using Raman micro-spectroscopy (MRS), energy dispersive X-ray micro-fluorescence (μ EDFRX) and Fourier transform infrared spectrometry (FTIR-ATR). The first two are non-destructive techniques and, in the case of FTIR-ATR, the amount required is very small, which allows the information to be obtained without the need to destroy the entire decoration. Through the coordinated application of the three techniques, it is possible to determine aspects related to the mineral and elemental composition of the samples, as well as to obtain information, thanks to the use of FTIR-ATR, about the temperatures to which they may have been subjected (Odriozola and Hurtado 2007; Jones et al. 2019). The use of μ EDXRF elemental analysis to generate surface maps should be highlighted as they clearly clarify the presence and distribution of characteristic chemical elements.

The application of these techniques to the study of white paste has been shown to offer precise and interesting results, although they have never been used together for the type of decoration being looked at here. There are, however, references for other types of decoration and pigments in which their efficacy has been demonstrated (Akyuz 2012; Tuñón et al. 2016; Tuñón et al. 2020).

2. Sampling

For this study, five pottery sherds (Table 1) and two horn fragments used as reference samples were analysed. Two of the sherds (BE-219-1 and BE-144) are held in the Museum of Jaén and authorisation was not granted to extract a minimum amount of white paste. The small sample selected is due to the uniqueness of this type of decoration both in Peñalosa and, in general, in the southeast of the Iberian Peninsula during the Bronze Age.

The pottery was very fragmented, hindering determination of the original typology. All the sherds were decorated on their surfaces with motifs filled with white paste, which, although not fully preserved, were sufficiently clear to be identified and analysed. The decorative techniques used consisted of exterior impressions (BE-28570, BE-28497-2, BE-144 and BE-219-1), interior and exterior impressions (BE-28508) and exterior incisions (BE -219-1). The decorative motifs were herringbone, circle and zigzag shapes with alternating horizontal and oblique lines (Figure 2). These techniques and decorative motifs were classified within the proto-Cogotas pottery type, which developed during the Full Bronze Age on the Iberian Peninsula (Arteaga and Schubart 1982; Schubart and Ulreich 1991; Abarquero 2005).



Figure 2. Analysed pottery decorated with white paste inlays (a) BE-28570; (b) BE-219-1 (c) BE-144; (d) BE-28497-2; (e) BE-28508.

The sherds came from different dwelling units, as well as from different chronocultural phases of Peñalosa. Three were associated with domestic contexts (BE-28497-2, BE-28570, BE-28508) and the other two (BE-219-1 and BE-144) were found in surface levels next to Tomb 12, an isolated and highly eroded structure on the western slope of the settlement (Figure 1) (Contreras et al. 2000).

Chronologically, three of them (BE-219-1, BE-144; BE-28570) belong to Phase IIIA (1950/1900-1750/1700 Cal BC), corresponding to the full period and the peak of the site's occupation, while the other two (BE-28508 and BE-28497-2) are associated with Phase III0 (1600-1450 Cal BC), the latest phase documented to date at the Peñalosa archaeological site.

Sample	Type	Context	Chronology	Technique	Decoration	Analysis
BE-28570	NI	Domestic	Phase IIIA	Impressed	Herringbone	MRS, μ EDXRF, FTIR-ATR
BE-219-1	Carinated vessel	Surface, near Tomb 12	Phase IIIA	Incised	Circle	MRS, μ EDXRF
BE-144	Carinated platter	Surface, near Tomb 12	Phase IIIA	Impressed	Zigzag	MRS, μ EDXRF

BE-28497-2	NI	Domestic	Phase III0	Impressed	Zigzag	MRS, μ EDXRF, FTIR-ATR
BE-28508	NI	Domestic	Phase III0	Impressed	Bands of horizontal lines and herringbone	MRS, μ EDXRF, FTIR-ATR

Table. 1. Pottery analysed. NI (not identified).

Two deer (*Cervus elaphus*) antler fragments, one without thermal alteration (BE-25308) and the other with calcination traces (BE-25405-5), were also analysed (Figure 3). Both were used as reference samples in the composition study of the white paste that may have been manufactured with this raw material. It should also be added that the calcination of the antlers results in an intense white colouration very similar to that of the white paste fillings; thus the study of the firing temperature of these bone remains using FTIR-ATR will allow links to be established with the manufacture of the white paste of the pottery vessels.

The selection of deer antlers rather than other faunal finds from the settlement is also supported by several aspects that attest to the importance of this bone element. Firstly, they are the only fauna remains with signs of calcination recorded in Peñalosa. Secondly, antlers appear to have been the preferred bone raw material, judging by their concentration in very specific areas of the settlement (Houses X and VI), unlike the rest of the recorded fauna, which is scattered throughout the archaeological site.

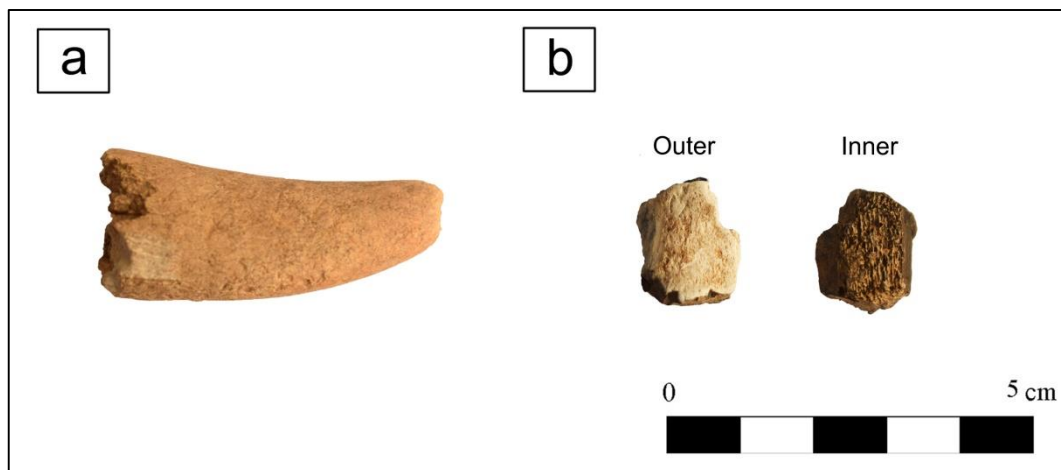


Figure 3. Fragments of deer antler analysed. (a) BE-25308, (b) BE-25405-5.

3. Methods

MRS and EDXRF could have been applied to all the white paste samples and antler fragments. However, as already indicated, it was not possible to subject samples BE-219-1 and BE-144, deposited in the Museum of Jaén, to FTIR-ATR analysis.

3.1. Micro Raman Spectroscopy (MRS)

This technique was applied according to the method described in Sánchez et al. (2019) and Tuñón et al. (2020). A Renishaw ‘in via’ Qontor Spectrometer coupled with a confocal Leica DM LM microscope (CICT, University of Jaén), equipped with a Nd:YAG laser (532 nm, 50 mW) and a diode laser (785 nm, 300 mW), and a Peltier-cooled CCD detector, calibrated to the 520.5 cm^{-1} line of silicon were used. The maximum laser output power was eventually reduced using neutral density filters. The spectra were acquired using the 50 \times objective in the 100 to 3200 cm^{-1} region, with a spectral resolution of ca. 1 cm^{-1} (2,400 lines/mm grating in 532 nm laser) and ca. 1 cm^{-1} (1,200 lines/mm grating in 785 nm laser). Acquisition time was set between 1 and 10 s per accumulation and the maximum number of accumulations was 50.

3.2. Micro energy dispersive X-ray fluorescence (μ EDXRF)

This technique was also applied according to the method described in Tuñón et al., (2020). An energy dispersive X-ray microfluorescence spectrometer (M4 Tornado, Bruker Nano) was used for this paper (CICT, University of Jaén). This spectrometer was equipped with a microfocus X-ray tube with an Rh anode, a polycapillary lens for X-ray focusing, and a 30- mm^2 energy dispersive detector (SDD) calibrated to $\text{K}\alpha_1$ line of Zr standard (15.775 keV). The sample chamber (200 x 160 x 120 mm) incorporated an XYZ motorised stage (330 mm x 170 mm) for sample positioning. A high resolution microscope (10x, 100x) was used to position the sample at the desired distance from the polycapillary. To increase the sensitivity of the low Z elements, the sample chamber could be brought under vacuum (20 mbar). For the analysis of the samples a spot size of 25 μm was chosen at an operating X-ray tube voltage of 50 kV (30 W) and a current of 600 μA .

The concentration values were obtained with Bruker’s ESPRIT software (version 1.5) which included a standardless quantification option (MQuant) based on a fundamental parameter method allowing a large variety of samples to be quantified. Semiquantitative analysis was performed by calculating a theoretical spectrum with the Sherman equation with correction of matrix effects. This calculated spectrum was compared to the measured one and then the quantification result was iteratively improved (Rousseau, 2004; Bruker, 2013; Flude et al., 2017). Reference samples (different from those commonly used for the standard calibration and maintenance of the instrument) were not used in this study due to the heterogeneity of the sample composition.

Two measurement methods were applied for μ EDXRF analysis:

- Mapping analysis. This type of analysis is ideal for determining the concentration and distribution of chemical elements on the pottery surface, making it possible to visually define the compositional differences between the ceramic paste and the decoration. The main mapping experimental parameters were adjusted for each mapping: step size (50 μm) and dwell time (2-5 ms/pixel). Map dimensions were changed according to the size of each analysed figure.
- Single-spot analysis. This measurement type allowed the chemical composition of the pottery and white pastes to be determined at specific points. At least, three measurements of 120 s were carried out on both the ceramic paste and the white paste. High resolution microscopy coupled to the μ EDXRF equipment

allowed further delineation of the areas so as to avoid sectors with discontinuous or fragmented decoration.

3.3. Fourier transform infrared spectroscopy-Attenuated total reflectance (FTIR-ATR)

FTIR spectra were collected with a Jasco 6200 spectrometer (CIC, University of Granada) with Attenuated Total Reflectance (ATR) in absorbance mode; 32 scans for each spectrum were acquired in the range 4000–400 cm^{-1} , with a spectral resolution of 4 cm^{-1} . Spectral analysis was performed using the Spectra Manager v2 software.

4. Results

The analytical techniques used (MRS, μEDXRF and FTIR-ATR) allowed a good to the composition and type of material used in the white paste fillings of the Peñalosa proto-Cogotas-type decoration. One of the materials identified was bone and the other was a type of clay, presumably one rich in kaolinite.

4.1. White paste inlays made from bone

In four of the five pottery samples (BE-28497-2, BE-28508-1, BE-28570, BE-144), the Raman spectra obtained all show the main ν_1 vibrational band position at $\sim 961 \text{ cm}^{-1}$, suggesting the presence of hydroxyapatite in the white paste (Figure 4) (Antonakos et al., 2007; Farooq et al. 2013; Freire et al. 2015; Garskaite et al. 2014). In an uneven manner, peaks of much lower intensity that are characteristic of hydroxyapatite appear at $\sim 434 \text{ cm}^{-1}$ and $\sim 593 \text{ cm}^{-1}$. In the case of Sample BE-144, an additional band is visible at 3575 cm^{-1} and is attributed to an OH vibration indicating the formation of well crystallised hydroxyapatite. Carbonate ions are also present at ~ 1034 , ~ 1050 , and $\sim 1076 \text{ cm}^{-1}$ and allow the biogenic nature of hydroxyapatite to be established when these peaks are present in the bone apatite structure (Bordes 2019) (Table 2). In any case, the differentiation between the types and the geological and biological origin of hydroxyapatite is still complex (Thomas et al. 2011).

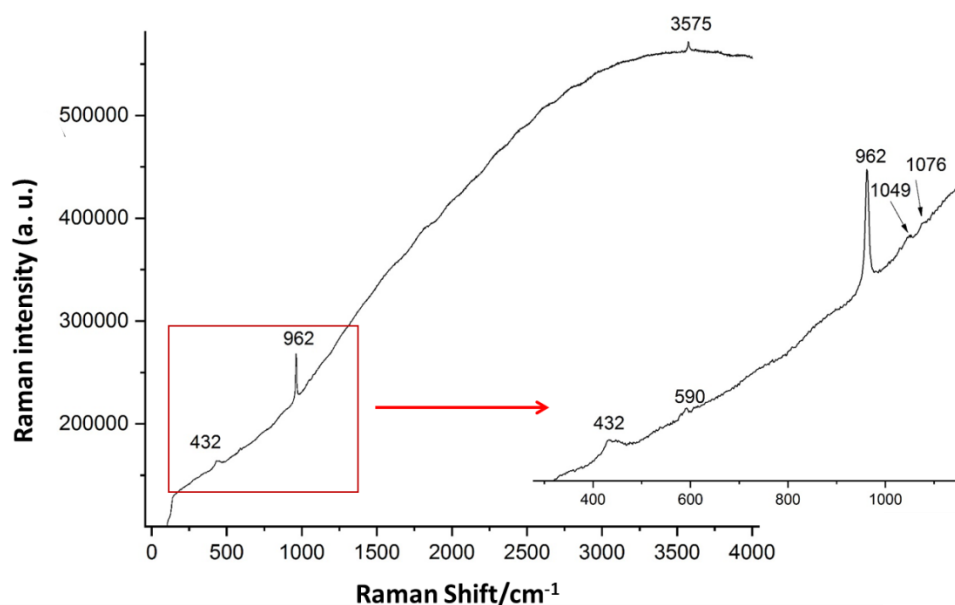


Figure 4. MRS results. Sample BE-144. Experimental conditions: 50x objective, 50 accumulations of 10 s, 532 nm argon ion laser, 2.5 mW.

In the case of the two antlers, the main Raman band of hydroxyapatite at $\sim 960\text{ cm}^{-1}$ was also identified. Furthermore, in the non-thermally altered horn (BE-25308) the peaks at $\sim 434\text{ cm}^{-1}$ and $\sim 593\text{ cm}^{-1}$ and the carbonate peak at 1074 cm^{-1} were identified. The calcined sample (BE-25405-5) also presented on the less burned side the typical spectrum of amorphous carbon formed during the combustion process (Coccatto et al. 2015; Bordes 2019) with the bands at 1373 and 1604 cm^{-1} .

Sample	Material	Wavenumber/ cm^{-1}	Ref.
BE-28570	White paste	435, 445, 454, 961, 1075	1, 2, 3
BE-144	White paste	432, 590, 962, 1049, 1076, 3575	1, 2, 3, 4
BE-28497-2	White paste	433, 963	1, 2, 3
BE-28508	White paste	430, 447, 582, 961, 1048, 1075	1, 2, 3
BE-25308	Antler	433, 450, 593, 608, 961, 1074	1, 2, 3
BE-25405-5	Calcinated antler	961, 1072, less calcinated side: 1373, 1604	1, 2, 3, 4, 5

Table 2. MRS results. References: 1) Freire *et al.* 2015; 2) Garskaite *et al.* 2014; 3) Antonakos et al., 2007; 4) Bordes, 2019; 5) Coccatto et al., 2015

The μEDXRF elemental analysis of the pottery samples shed more light on the composition of the fillers. In the case of the four samples with hydroxyapatite, the results obtained through the point analysis by μEDXRF showed a difference in the composition between the white paste and the ceramic paste. A considerable abundance of CaO (48.41 to 50.23 wt%) and P₂O₅ (36.54 to 41.94 wt%) was observed, the SiO₂ (2.47 to 6.31 wt%) and Al₂O₃ (2.69 to 5.53 wt%) values being very low. The amount of CaO and P₂O₅ in these samples added up to more than 85% of the total elemental composition. This indicates that the white paste corresponds to a pure calcium phosphate phase (Odriozola and Hurtado 2005, 2007). The reference bone samples provided results similar to those of white pastes, although slightly higher, with CaO percentages ranging between 53.99 and 57.33 wt% and P₂O₅ between 33.54 and 38.24 wt%. These data allow us to associate the composition of these inlays with a bone-type material (Table 3).

Regarding the ceramic paste of these four samples, Al₂O₃ (19.35 to 24.86 wt%) and SiO₂ (58.97 to 61.04 wt%) presented much higher values. Both are typical and majority elements of clay, together with other elements with a minority presence, such as K₂O (3.18 to 5.76 wt%), Fe₂O₃ (6.08 to 8.72 wt%) and TiO₂ (0.84 to 1.96 wt%) (Centeno et al. 2012). In those parts of the pottery where white fillings were not found, the percentages of CaO fell until it became a minority element (1.41 to 1.77 wt%) and P₂O₅ almost disappeared, being reduced to values of less than 1.22 wt%. The almost residual appearance of the latter suggests that it may come from the raw material with which the vessel was made.

Samples (no. of measurements)	Na ₂ O	MgO	Al ₂ O ₃	SiO ₂	P ₂ O ₅	SO ₃	-Cl	K ₂ O	CaO	TiO ₂	Fe ₂ O ₃	Total (Wt%)
BE-28570_WP (3)	0.04	0.03	2.69	2.47	41.94	0.91	0.27	0.09	50.23	0.03	0.87	99.57
S.D.	0.04	0.03	1.35	1.34	1.42	0.28	0.10	0.10	1.80	0.04	0.88	
BE-28570_CP (3)	0.29	0.55	23.32	58.97	1.22	1.54	0.03	3.18	1.50	0.84	8.06	99.50
S.D.	0.47	0.12	2.16	2.42	0.40	1.90	0.05	0.56	0.34	0.16	0.83	
BE-219-1_WP (4)	0.01	0.59	29.88	54.62	0.00	0.33	0.19	8.57	1.20	1.37	2.95	99.70
S.D.	0.03	0.09	0.33	0.86	0.00	0.19	0.04	0.80	0.29	0.14	0.61	
BE-219-1_CP (3)	0.45	5.68	19.03	50.49	0.06	0.48	0.51	8.13	1.87	1.10	11.76	99.55
S.D.	0.10	0.31	0.45	3.98	0.11	0.12	0.38	0.26	0.33	0.33	2.91	

BE-144_WP (4)	0.04	0.30	5.53	6.31	37.19	0.62	0.33	0.22	48.67	0.04	0.44	99.68
S.D.	0.06	0.04	1.89	2.45	2.72	0.33	0.07	0.09	1.57	0.01	0.15	
BE-144_CP (3)	0.09	1.70	19.35	59.42	0.44	0.90	0.07	5.76	1.41	1.40	8.72	99.25
S.D.	0.16	0.27	2.10	5.03	0.15	0.22	0.04	2.19	0.44	0.44	2.01	
BE-28497-2_WP (3)	0.25	0.00	3.38	3.85	40.78	0.76	0.39	0.23	48.41	0.04	1.70	99.78
S.D.	0.27	0.00	1.75	1.48	1.39	0.15	0.03	0.15	2.35	0.02	0.60	
BE-28497-2_CP (3)	0.48	0.63	22.53	59.75	0.78	0.00	0.13	5.00	1.77	1.96	6.57	99.59
S.D.	0.83	0.14	2.36	3.81	0.25	0.00	0.01	3.76	0.32	2.24	2.28	
BE-28508_WP (3)	0.08	0.05	5.03	6.25	36.54	0.25	0.43	0.43	49.76	0.05	0.77	99.64
S.D.	0.10	0.05	2.54	3.87	3.37	0.24	0.11	0.56	3.91	0.06	0.38	
BE-28508_CP (3)	0.28	0.60	24.86	61.04	0.40	0.00	0.08	3.92	1.61	0.81	6.08	99.67
S.D.	0.32	0.27	2.79	1.75	0.37	0.00	0.06	0.52	0.30	0.40	0.70	
BE-25308_A (9)	0.11	0.22	3.58	3.53	36.76	0.00	0.09	0.12	53.99	0.02	0.94	99.37
S.D.	0.11	0.03	2.23	2.55	2.62	0.00	0.01	0.11	2.89	0.01	0.50	
BE-25405-5 CA out (6)	0.00	0.01	2.21	2.12	38.34	0.08	0.47	0.18	55.82	0.02	0.63	99.88
S.D.	0.00	0.02	1.53	1.65	2.51	0.04	0.10	0.18	1.43	0.03	0.63	
BE-25405-5 CA in (8)	0.26	0.19	3.44	3.50	33.54	0.13	0.25	0.20	57.33	0.06	0.81	99.71
S.D.	0.19	0.05	2.67	2.92	3.68	0.02	0.15	0.22	4.03	0.08	0.91	

Table 3. Results μ EDXRF analysis. WP: White paste. PC: Ceramic paste. A: antler. CA: calcinated antler.

Mapping of the pottery sherd surfaces clearly showed that the differences in the concentrations recorded in the point analyses have a clear spatial continuity. The concentration of P and Ca in the white paste incrustations stood out clearly, while on the rest of the pottery surface the predominant elements were Al and Si (Figure 5). The rest of the elements (Ti, Mg, Cl, K, Fe, S, Na) either appeared scattered throughout the ceramic paste, as they are a natural part of the clay, or they were not detected through mapping due to their low amount.

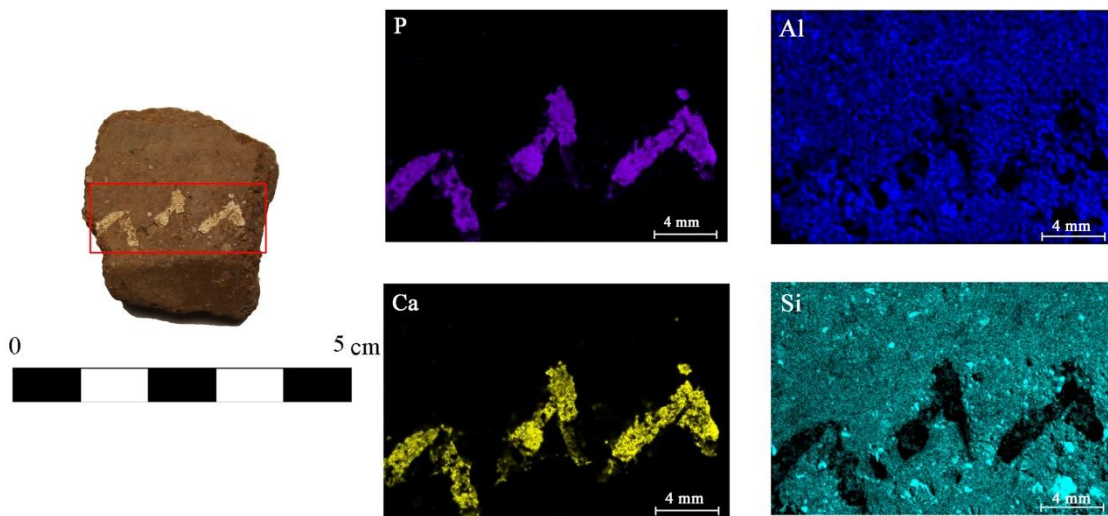


Figure 5. μ EDXRF mapping analysis of Ca, P, Al and Si in ceramic fragment BE-144.

Another parameter that allows this white paste to be associated with the biogenic nature of hydroxyapatite and, therefore, with bone matter, is the P/Ca ratio in the sample based on its elemental concentration (Table 4) (Odriozola and Martínez 2007). The P/Ca ratio found in the samples containing calcium phosphate was clearly above the limit proposed (1.98) by Schiegl et al. (2003) to distinguish between mineral and biogenic hydroxyapatite.

For their part, the analysed antlers showed a higher P/Ca ratio, reaching values close to 3%. The variability in the P/Ca ratio between the white pastes and the antlers may be

due to factors fundamentally justified by the various diagenetic processes that intervened in them. These processes can produce the enrichment or depletion of Ca and/or P (Douglas et al., 1992; Mamede et al. 2017), being particularly intensified especially in the case of the antlers. The porous structure of the antlers also makes them more susceptible to infiltration by other materials (Douglas et al., 1992), meaning that the postdepositional contributions received will be greater than in the case of white paste fillings, where grinding resulted in a dense and not very porous mass.

Sample	Ca	P	P/Ca
BE-28497-2	26.40	63.88	2.42
BE-28508-1	23.58	65.24	2.77
BE-28570	26.89	66.17	2.46
BE-144	25.01	65.60	2.62
BE-25308 (A)	23.19	68.81	2.97
BE-25405-5 (CA)	23.90	70.95	2.97

Table 4. Ca and P % weight elemental and P/Ca ratio. A: antler, CA: calcinated antler.

With regard to the FTIR-ATR analysis of the three pottery samples for which authorisation was obtained, the results added to our knowledge of the pottery and white filling manufacture.

In the case of ceramic paste, it was possible to determine the use of a siliceous clay, rich in clay minerals from the illite group, with siliciclastic tempers (Figure 6). The dominant bands in the IR spectra of the pottery were the SiO vibrations. These vibrations are related to illite and quartz and were common to all three samples (Table 4). Regarding these bands, peaks identified at 423-478 cm^{-1} refer to Si-O-Si bending vibrations associated with silicates (Erdoğan et al. 2016; Zviagina et al. 2020). Also, the main peak identified at 993-995 cm^{-1} (Figure 6) corresponds to the Si-O stretching vibrations of illite minerals. The doublet at 795-775 cm^{-1} due to Si-O symmetric stretching, and the peak at 693 cm^{-1} due to Si-O symmetric bending, show the presence of quartz (Saikia and Parthasarathy 2010; Shoval et al. 2011). Moreover, the 721 cm^{-1} peak due to Al-O-Si bending indicates the presence of albite (Cantelli et al. 2020).

The presence of bands characteristic of structural water indicates that this pottery was subjected to a firing temperature of lower than 700°C. Deformation vibrational modes of water molecules are present at 1644, 1636, and 1634 cm^{-1} (Erdoğan et al., 2016) (Figure 6). Moreover, wide and weak OH-stretching bands are present at 3450, 3623 and 3693 cm^{-1} (Frost and Mendelovici, 2006; Anbri et al., 2008; Elgamouz and Tijani, 2018). These OH vibrational bands disappear due to the loss of absorbed water at high temperatures, manifesting in lower vibrations in stretching modes, which begin to occur above 700°C (Elgamouz et al. 2019).

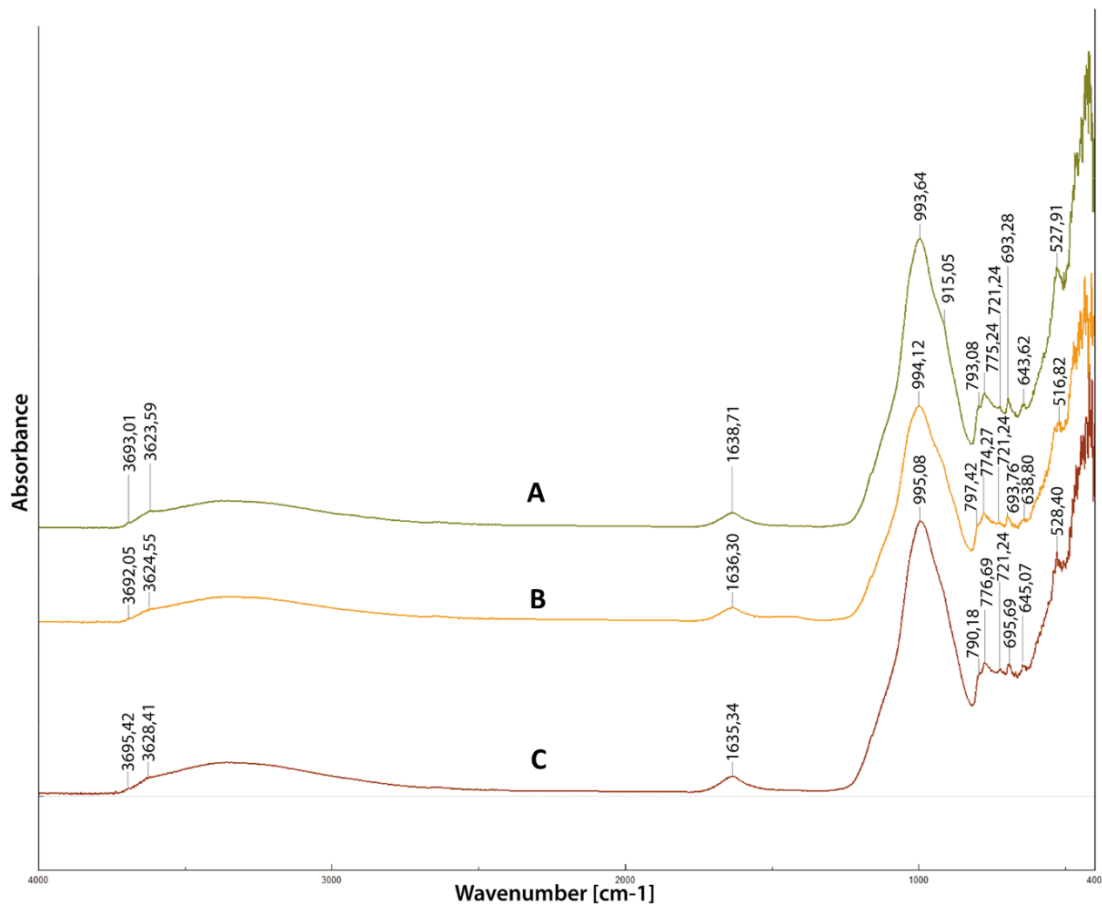


Figure 6. FTIR-ATR results. Ceramic pastes. A) BE-28570, B) BE28580, C) BE-28498.

The white paste spectra are all similar and are characterised by the presence of CO_3^{2-} bands at 1456 cm^{-1} , $1410\text{--}1411\text{ cm}^{-1}$ and 872 cm^{-1} , as well as bands associated with PO_4^{3-} located at 961 cm^{-1} and $598\text{--}599\text{ cm}^{-1}$ and 560 cm^{-1} (Odriozola and Hurtado, 2007; Giustetto et al., 2013; Perišić et al. 2016). These intensities show the presence of hydroxyapatite and carbonate-hydroxyapatite, both components of bone (Perišić et al. 2016). The band located at 3573 cm^{-1} belongs to the hydroxyl group (Giustetto et al. 2013; Thompson et al. 2013), which is also part of the bone composition. The bands situated in the $750\text{--}400\text{ cm}^{-1}$ region correspond to the stretching and bending modes of phosphate groups of hydroxyapatite (Odriozola y Hurtado 2005, 2007).

The previous bands were also present in the antlers analysed. Only the band located at 1956 cm^{-1} in the antlers moved at lower intensities or disappeared in the white paste fillings. There was also a displacement between 1450 and 1456 cm^{-1} between the calcined antler (BE-25308) and the non-thermally altered antler (BE-25405). These displacements occur as a consequence of exposure to high temperatures (Lebon et al., 2008) (Figure 7).

The attribution of the bands obtained to biogenic hydroxyapatite makes it possible to rule out a geological nature for the hydroxyapatite. In that case, the band at 574 cm^{-1} would be more intense and the band at 560 cm^{-1} would appear as a shoulder of this main band. However, in the biogenic apatites, the main band appeared at 560 cm^{-1} (Odriozola and Hurtado 2005, 2007) and the band disappeared at 574 cm^{-1} , as occurred with the white paste fillings studied. On the other hand, the lack of another type of band

unrelated to the composition of the bone indicates that only this material was used for the manufacture of white pastes.

In terms of the firing temperature, there were some indicators that the white paste samples had been heated. In general, in non-calcinated bones the band at 1640 cm^{-1} was more intense and related to H_2O bending vibration modes, which, in addition, formed a broad band around 3360 cm^{-1} (Giustetto et al. 2013). In the case of white pastes and calcined bone, the band at 1640 cm^{-1} lost intensity or disappeared and a new band emerged at 3573 cm^{-1} (Figure 7).

Further proof of heating was the 2013 cm^{-1} band identified only in the white pastes. This band was defined as cyanamidapatite (Starkovich et al. 2013), which some researchers suggest arises when calcined bone comes into contact with charcoal during firing (Hüls et al. 2010; Van Strydonck et al. 2010).

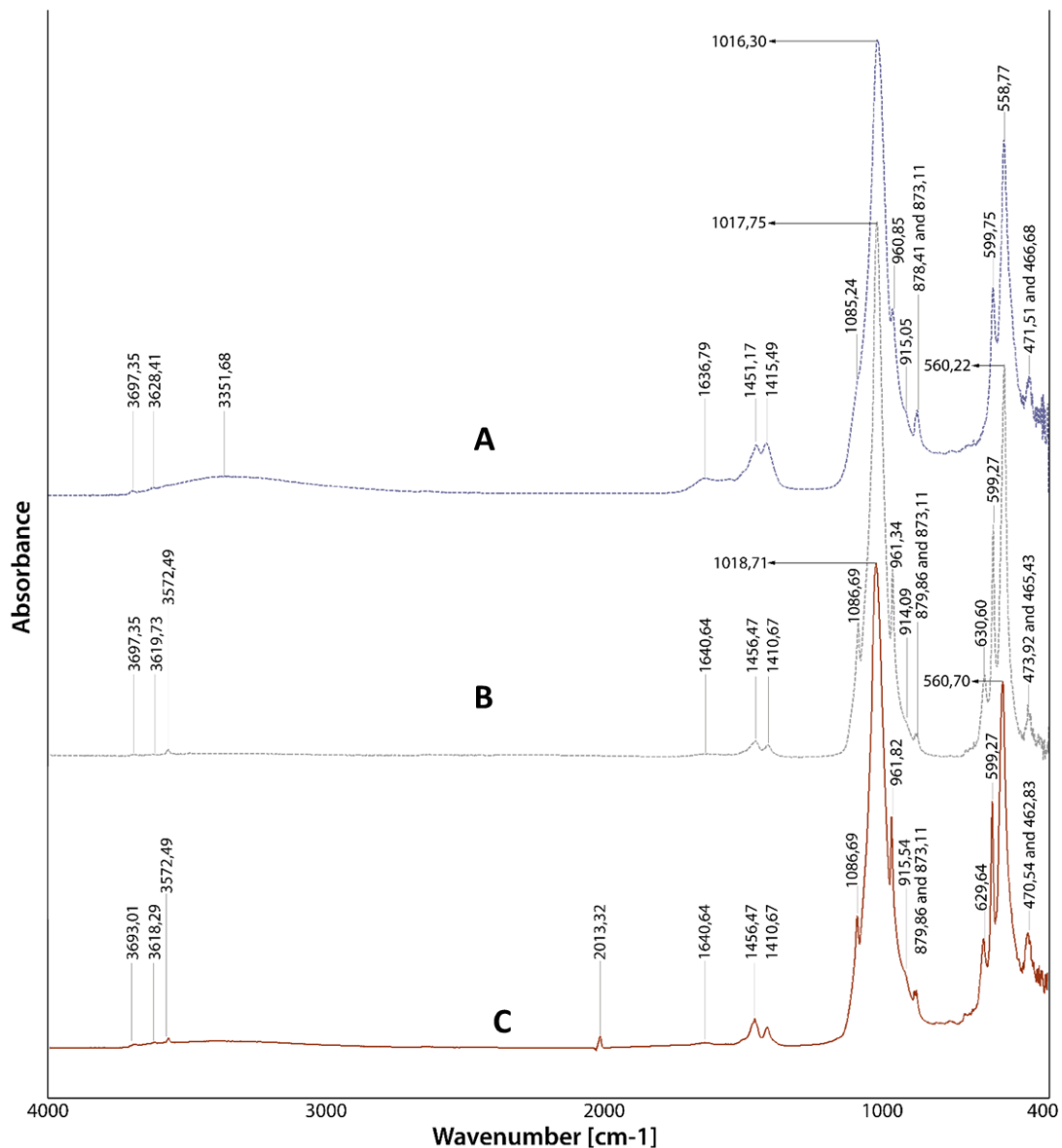


Figure 7. FTIR-ATR results, A) Deer antler, B) Calcinated deer antler, C) White paste inlay, sample BE-28498.

On the other hand, the band at 630 cm^{-1} appears when the bone mineral (hydroxyl apatite carbonate) transforms into a crystalline phase (hydroxyapatite) and its appearance occurs when the bone has been calcined at high temperatures (between 700 and $900\text{ }^{\circ}\text{C}$) (Perišić et al. 2013). Likewise, the good definition of the PO_4^{3-} bands indicates that the bones were heated to a high temperature, a phenomenon that usually occurs above 800°C , when the water and organic content of the bone has been lost and its crystalline structure is reorganised (Perišić et al. 2016; Thompson et al. 2013). Furthermore, amorphous calcium phosphate has a well-defined doublet between 500 and 600 cm^{-1} in well crystallised hydroxyapatite, as observed in the analysed white pastes (Wright and Schwarcz 1996; Pucéat et al. 2004; Munro et al. 2007).

In the antler that had not been thermally altered (BE-25308), a band between 1600 - 1660 cm^{-1} was recorded and can be linked to the presence of organic elements and water (Thompson et al. 2013). This band lost intensity in the calcined horn (BE-25405) and white paste fillings (BE-28570, BE-28508-1, BE-28497-2 PB), due to the disappearance of organic elements and structural water in temperatures above 800°C (Holck 2005; Walker et al. 2008; Mamede et al. 2017: 5, Marques et al. 2018). The band at 1085 cm^{-1} , a shoulder in the rest of the non-thermally altered horn, developed in a peak of the antisymmetric ν_3 mode of hydroxylapatite at 1086 cm^{-1} (Merincea et al. 2004) only identified in the calcined fragment and in white paste. At 900°C , the OH stretching band at 3570 cm^{-1} also appears markedly (Goldberg et al. 2020) in white paste and calcined horn.

4.2. White paste inlays with kaolinite clay

The Raman analysis of the white paste of sample BE-219-1 did not present a resolatory spectrum. Despite the above, the absence of the Raman signal of minerals that can be easily identified with this technique and used in the production of white paste (calcite, talc, gypsum or dolomite) allows us to limit the search for the materials responsible for the white colouration of the inlaid paste (Middleton et al. 2005; Buzgar and Apopei 2009; Buzgar et al. 2010; Centeno et al. 2012).

Thanks to the μEDXRF point and surface analysis, the sample presented a composition that was clearly different to the rest of the samples (Table 3). In the white paste there was an obvious low presence of P and Ca and its composition was similar to that of the clay that makes up the ceramic paste. However, the most relevant and differentiating data are a higher concentration of Al and Si (Figure 8). The rest of the elements that made up the white paste (Ti, Mg, Cl, Fe, S, Na) did not present notable surface maps due to their low quantity and/or the similarity of concentration with the ceramic paste. The data obtained would therefore indicate that the origin of the white paste in this pottery is a white clay that, judging by the high values of Si and Al, would have been rich in kaolinite (Buzgar et al. 2010, 2013).

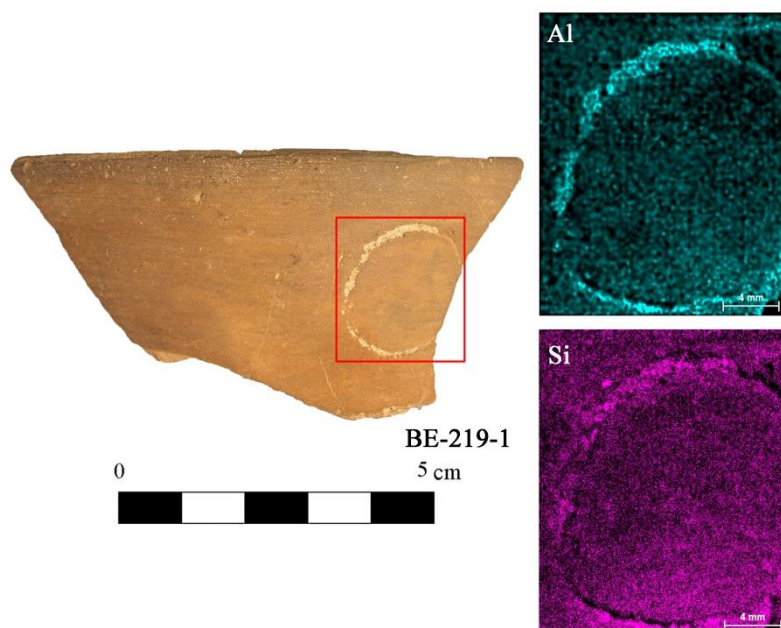


Figure 8. μ EDXRF mapping analysis of Ca, P, Al and Si in ceramic fragment BE-219-1.

The enrichment of this white paste with K_2O (8.8 wt%) can be linked to the origin of the raw material itself. In the surroundings of Peñalosa, K_2O can be associated with feldspars found as a contribution to the kaolinitic clays from the erosion of kaolinised granites (IGME 1977).

On the other hand, the concentration of Fe_2O_3 and MgO on the ceramic surface of Sample BE-219-1 was much greater than in the white paste. The presence of these oxides in the white filler can be associated with impurities in the kaolinitic clay itself. The existence of Fe_2O_3 in the crystal lattice of kaolinite can affect its whiteness (Cameselle 1995: 291); hence the colour of this paste is less whitish than those made with bone and it takes on a more yellowish hue.

In relation to the other four pieces of pottery analysed, the high values of Fe_2O_3 and MgO in the ceramic paste of sample BE-219-1 suggest that the clay used to manufacture it had a different origin. These elements are typical of red clays, which can be easily found in the Peñalosa area (García González et al. 2010) as a product of the erosion of different rock formations, such as sandstones or slate (IGME 1977).

4. Discussion

In the first place, it is evident that the pottery assemblage analysed is limited, not so much by an incomplete selection, as by the exceptionality of this type of decoration at the Peñalosa archaeological site. Secondly, the impossibility of minimally altering the white paste with the application of FTIR-ATR in two of the samples prevented the selected analysis methodology (MRS+ μ EDXRF+FTIR-ATR) from being fully or systematically applied. Despite this, several aspects of the results obtained in the analysis of the pottery and the white pastes of the inlays can be discussed and commented on: composition, manufacture, origin and relationships that can be established with other regions on the Iberian Peninsula.

In four samples (BE-28497-2, BE-28508-1, BE-28570, BE-144) the clear identification of biogenic hydroxyapatite indicates that bone was the material of choice for the production of white paste. Its use is documented in the two chronological phases that span the first half of the second millennium BC. In terms of the rest of the components that make up these white pastes, experimental studies carried out on different anatomical parts and different animal species (Buddhachat et al. 2016) show that they may contain these minority elements. Elements such as Al, Si, K, S, Mg, Ti and Fe are found in the bones of many animal species, as is also demonstrated by the values obtained in the reference antler samples analysed in this study (Table 3). However, from the elemental chemical composition of the bone it is difficult to know which animal species it comes from. This is due to the fact that there is no fixed pattern among species in the percentage of these chemical elements, as their proportion may vary depending on the calcification of the bone tissue and the age and sex of each individual (Odriozola and Martínez 2007). Furthermore, structurally there are similarities between certain species, as in the case of bovine and human bones (Herliansyah et al. 2009). It should also be taken into account that the presence of some lightweight elements such as S and Cl on the surface may be due to interaction with the environment, sediment and/or the cleaning procedure (Centeno et al. 2012; Angeli et al. 2019: 194).

Another important aspect to ascertain is whether this bone component was heated in a first firing together with the pottery or whether it was heated separately and later added to the cavity made for the decoration. Some studies (Baldini et al. 2005; Všíanský et al. 2014; Kos et al. 2015; Jones et al. 2019) have proposed that the bone was thermally altered before being crushed or ground for adhesion as a component in the white paste, while other researchers have demonstrated the friability of burnt bone at high temperatures (Munro et al. 2007). In other research it has been argued that the bone would have been added unprocessed and fired with the pottery to allow the organic matter to adhere to the pottery surface (Odriozola and Hurtado 2007; Giustetto 2013; Jones 2019).

In the case of Peñalosa, the ceramic paste in which the white paste was embedded was made with a siliceous clay rich in minerals from the clay of the illite group and with siliciclastic tempers. The data provided by the FTIR-ATR analyses indicate a firing temperature of below 700°C. This contrasts with the temperature of above 800°C reached when making the white paste that coincides with the estimated firing temperature for calcined horn (BE-25405-5). Therefore, it seems clear that there were two separate manufacturing processes. The final phase would have been the embedding of the white paste in the pottery, although we are unable to ascertain whether there was a subsequent short firing with the two components together.

It is also necessary to take into account the possible alterations caused by the use of the vessel itself or by postdepositional agents that have acted on them (Thomas et al. 2011). In any case, the lack of evidence of this type of activity or process in the samples analysed, as well as the poor definition of the pottery shapes due to the small size of the sherds bearing this type of decoration, makes it difficult to assign possible thermal alterations to a specific use of the vessel. On the other hand, throughout the research it has been defended that this decorated tableware was associated with household goods intended for food consumption and, due to its aesthetic qualities, reserved for special occasions (Harrison 1995; Abarquero 2005). Furthermore, in the event that any type of alteration had been caused by the use and burial of the pottery, it would not have been

enough to produce these thermal transformations in the white paste (Odriozola and Hurtado 2007). Therefore, only the pottery firing could have modified the bone structure.

Moreover, these white pastes have a very whitish colouration that can only be obtained with calcined bone. This is because, as the temperature increases, the bone progressively takes on a lighter colour (from light grey to white). When the bone calcines, it takes on the intense white colour typical of hydroxyapatite (Bonucci and Graziani 1975; Giustetto et al. 2013; Lim et al. 2014), as is the case of the white incrustations under study. For this characteristic to occur in the bone, the heating had to have reached 800°C (Walker et al. 2008; Mamede et al. 2017: 5, Marques et al. 2018; Lambrech and Mallol 2020). In this respect, in Peñalosa only deer antlers have been shown to have reached such temperatures (Contreras, 2000; Sanz and Morales 2000; Altamirano, 2015).

The possible use of deer antlers in the preparation of the white inlays of the Peñalosa pottery also has very clear archaeological support. Of note, as already indicated, is the concentration of debris from shed deer antlers found in Houses VI and X at Peñalosa, which were purposely calcined to serve in the manufacture of different tools, particularly the handles. It seems evident, therefore, that the inhabitants of Peñalosa were aware of the benefits of heating this raw material to make it easier to work with.

Due to their hardness and elasticity, the use of deer antlers for the manufacture of utensils is widely documented in prehistory (Schibler 2001; Kos et al. 2015; López Padilla 2019; Gummesson et al. 2019) and was especially widespread in the Argaric territory (Altamirano 2015). The choice of deer antler for the manufacture of white paste inlays has also been documented in other contexts chronologically contemporaneous with Peñalosa, such as Podunavlje (Croatia) (Kos et al. 2015).

In the case of Sherd BE-219-1, dated to the first quarter of the second millennium BC, the raw material used to make the white paste was a clay rich in kaolinite. This mineral is not particularly common in this area, but can be found in the igneous rocks, such as granites, located approximately 6 km northeast of the Peñalosa archaeological site. It has been incorporated into the rock structure by volcanic, hydrothermal or weathering processes (Bartolomé 1997) (IGME, 1977).

Determining the conditions and approximate firing temperature of the kaolinitic white paste is more complicated with the analytical techniques used and given the impossibility of analysing it by FTIR-ATR. In this regard, the studies undertaken suggest two hypotheses: that these white pastes were hardened simply by letting them dry (Všianský et al. 2014) or that they were heated together with the pottery in a second low temperature firing (below 500°C) (Lantes-Suarez et al. 2010).

Finally, the use of two types of filling in the early second millennium BC in the Peñalosa pottery could be due to two factors: on the one hand, different manufacturing methods justified by the procedures of different artisans, or, on the other, various external influences on the production of the Peñalosa white pastes.

In the first case, if the existence and supply of deer antlers is demonstrated at Peñalosa, for the application of white clay there would have had to have been a well-defined

supply strategy that would have allowed a white pigment that stood out over the rest of the pottery to be obtained as an end product. In this respect, kaolinite is not an abundant resource in the area around the archaeological site. If the foregoing is verified, it would be evidence of a more complex pottery production and specialisation (Aranda 2010). However, to date the archaeological record only contains one analysed fragment found to have this composition, so it is difficult to assert whether this type of manufacture is associated with local or foreign production.

In the second case, it has been proposed that there was a greater exchange of ideas when a settlement was located at the distribution limit of different technical identities or border areas (Odriozola 2018). In this respect, Peñalosa is an enclave located in a border area in contact with both the central Meseta and the southeast of the Iberian Peninsula; therefore it would have been subjected to various influences that could have met the requirements proposed in the aforementioned study. The white paste fillings made with bone have shown parallels both in temporality (Aubert et al. 1983; Abarquero 2005) and composition with the productions of the Middle Guadiana River area, where those made with this type of material are concentrated, whereas in the northern Meseta area the composition of these decorations is predominantly calcite (Odriozola et al., 2012). Although the existence of this influence from the southwest of the Iberian Peninsula is evident, the manufacturing technology of this pottery (Vico 2021) and the evidence of the working of certain bone resources at the archaeological site itself, suggests that this type of production was local.

The use of bone in the manufacture of these decorative fillings is widespread in other European Bronze Age contexts (Gherdán et al. 2003, Sziki et al. 2003, Roberts et al. 2008; Parkinson et al. 2010; Kos et al. 2015; Sofaer and Roberts 2016), meaning that the Peñalosa settlement followed patterns very similar to the predominant manufacturing model during that period over a wide territory.

Another contact route would have been via the southern Meseta, where there are large kaolinite outcrops (IGME 2005) that could also have been used in the manufacture of white paste decorations, as attested by the case of BE-219. In the northwest of the Iberian Peninsula, white paste decorations have also been identified in Bell Beaker pottery from the Copper Age in Finisterre (Galicia) (Covertini and Querré 1998; Lantes-Suárez et al 2015) composed of kaolinite. However, in this area, no proto-Cogotas type pottery from the Bronze Age that would allow the results to be compared has been documented. Outside this territory, at the archaeological site of San Cristóbal (Cáceres), the researchers maintain that the white pastes of the Bell Beaker pottery were made with kaolin (González and Barroso 1996-2003) and that perhaps there may have been a production tradition throughout time. Since these authors do not contrast their hypothesis with any type of archaeometric analysis, their proposal cannot be validated. However, the use of this raw material for the manufacture of white paste does not confirm the external origin of this example, since, as previously mentioned, this mineral can be found in secondary deposits in the area of the archaeological site. For the time being, the Peñalosa pottery appears to be almost unique in the Bronze Age, pending new finds and archaeometric analyses that would allow external relationships or local productions to be established.

5. Conclusions

The application of the MRS, μ EDXRF and FTIR-ATR techniques to the study of the white paste inlays of Peñalosa Bronze Age pottery has proven useful in identifying the nature of the raw material and some of the technical processes used in their manufacture. The use of μ EDXRF surface analysis was particularly innovative.

It was possible to establish that the white paste fillings in the pottery were manufactured with two different types of material, bone and kaolinite, both used contemporaneously. A greater technological and decorative homogeneity was observed in the pastes that present biogenic hydroxyapatite, while the white paste made with kaolinite differed from the rest.

The comparison of the analytical results obtained in the case of white pastes of bone origin and the archaeofaunal and contextual studies was also of great interest. Thanks to these, it was possible to hypothesise on the type of bone used for the manufacture of these decorations. They indicate that the potters made a very specific and conscious selection of the raw material, in this case presumably deer antlers.

In summary, this study has provided a broader perspective on the production technology used to make the white paste inlays of the proto-Cogotas-type pottery of the Bronze Age Argaric culture in the southeast of the Iberian Peninsula. No studies of this type had previously been carried out in this area. However, in future research it will be necessary to increase the number of samples, expanding at the same time the geographical area studied in order to draw more precise conclusions regarding the evolution and transfer of the manufacturing technology of these decorations.

Acknowledgments

This article has been funded by the Archaeometric Studies Unit of Excellence, “Inside the Artefacts and Ecofacts” of the University of Granada Research and Transfer Plan, and the University Research Institute for Iberian Archaeology. We are grateful for the support shown by the Centre for Technical Scientific Instrumentation of the University of Jaén and the Centre for Scientific Instrumentation of the University of Granada. Finally, We are grateful to the Museum of Jaén for having made it easier to provide us with the materials, especially from its director Francisca Hornos Mata and her curator Carmen Repullo,

5. Bibliografía

Abarquero, F.J., 2005. Cogotas I. La difusión de un tipo cerámico durante la Edad del Bronce. *Arqueología en Castilla y León. Monografías Junta de Castilla y León. Conserjería de Cultura y Turismo.*

Akyuz, S., Akyuz, T., Emre, G., Gulec, A., Basaran, S., 2012. Pigment analyses of a portrait and paint box of Turkish artist Feyhaman Duran (1886-1970): The EDXRF, FT-IR and micro Raman spectroscopic studies. *Spectrochimica Acta Part A: Molecular and Biomolecular Spectroscopy* 89, 74-81. <https://doi.org/10.1016/j.saa.2011.12.046>

Altamirano, M., 2015. Evidencias de extracción de soportes como método para la elaboración de artefactos óseos durante el II milenio AC en la Península Ibérica. *Marq. Arqueología y Museos* 6, 35-43.

Antonakos, A., Liarokapis, E., Leventouri, T., 2007. Micro-Raman and FTIR studies of synthetic and natural apatites. *Biomaterials*, 28, 3043-3054.
<https://doi.org/10.1016/j.biomaterials.2007.02.028>

Aranda, G., 2010. Entre la tradición y la innovación: el proceso de especialización en la producción cerámica argárica. *Menga* 1, 77-95.

Anbri, Y., Tijani, N., Coronas, J., Mateo, E., Menendez, M. 2008. Clay plane membranes: development and characterization. *Desalination* 221, 419.
<https://doi.org/10.1016/j.desal.2007.01.101>

Angeli, L., Brunetti, A., Legnaioli, S., Fabbri, C., Campanella, B., Lorenzetti, G., Pagnotta, S., Poggialini, F., Palleschi, V., Radi, G., 2019. Analysis of the middle Neolithic trichrome pottery: Characterization of the decorelaciónn using X-Ray fluorescence and Raman spectroscopy. *J. Arch. Sci.* 24, 192-197.
<https://doi.org/10.1016/j.jasrep.2019.01.008>

Arteaga, O., Schubart, H., 1980. Fuente Álamo. Excavaciones de 1977. *Noticiario Arqueológico Hispánico* 9, 245-291.

Aubet, M^a. E., Serna, M^a R., Escacena, J.L. y Ruíz, M., 1983. La mesa de Setefilla. Lora del Río (Sevilla). Campaña de 1979. *Excavaciones Arqueológicas en España*, 122, Ministerio de Cultura, Madrid.

Baldini, M.I, Cremonte, M.B., Lía, I., Díaz, M.A., 2005. De felinos, pastas y pigmentos. La cerámica de Choya 68 desde una perspectiva arqueométrica. In: Martín, S.E. and Gonaldi, M.E (Eds.), *La cultura de la aguada y sus expresiones regionales*. Secretaría de Ciencia y Tecnología. Universidad de la Rioja, Logroño, pp. 87-105.

Bartolomé, J.F., 1997. El caolín: composición, estructura, génesis y aplicaciones. *Boletín de la sociedad española de cerámica y vidrio* 36 (1), 7-19.

Bonucci, E., Graziani, G., 1975. Comparative thermogravimetric X-ray diffraction and electron microscope investigations of burnt bones from recent, ancient and prehistoric age. *Atti dell'Accademia Nazionale dei Lincei, Rendiconti, Classe di Scienze Fisiche, Matematiche e Naturali* 59, 517-532.

Bordes, L., 2019: *Analysing Micro-residues on Prehistoric Stone Tools by Raman Microscopy and Determining Ther Origins*. PhD thesis. Unviersity of Wollongong, Australia.

Bruker Nano GmbH. M4 Tornado. High performance Micro-XRF spectrometer 2013. User manual, ed. Bruker Nano GmbH. Berlín.

Buddhachat, K., Klinhom, S., Siengdee, P., Brown, J.L., Nomsiri, R., Kaewmong, P., Thitaram, C., Mahakkanukrauh, P., Nganvongpanit, K., 2016. Elemental Analysis of

Bone, Teeth, Horn and Antler in Different Animal Species Using Non-Invasive Handheld X-Ray Fluorescence. PLoS ONE 11(5), e0155458. <https://doi.org/10.1371/journal.pone.0155458>

Buzgar, N., Apopei, A.I., 2009. The Raman study of certain carbonates. *Analele Stiintifice de Universitatii A.I. Cuza din Iasi. Sect. 2, Geologie (2)*, 98-112.

Buzgar, N., Bodi, G., Buzatu, A., 2010. The raman study of white, red and black pigments used in cucuteni neolithic painted ceramics. *Geologie VI (1)*, 5-14.

Cameselle, C., Núñez, M.J. Lema, J.M., Pais, J., 1995. Leaching of iron from kaolins by a spent fermentation liquor: influence of temperature, pH, agitation and citric acid concentration. *J. Industrial Microbiology* 14, 288-292.

Cantelli, M., Facchi, A., Izzo, F.C., Zendri, E., 2020. Characterization of Etruscan non-vascular ceramic fragments, in: 2020 IMEKO TC-4 International Conference on Metrology for Archaeology and Cultural Heritage Trento, Italy, October 22-24, 2020. pp. 585–589.

Centeno, S.A., Williams, V.I., Little, N.C., Speakman, R.J., 2012. Characterization of surface decorrelaci3ns in Prehispanic archaeological ceramics by Raman spectroscopy, FTIR, XRD and XRF. *Vibrelacionnal Spectroscopy* 58, 119-124. <https://doi.org/10.1016/j.vibspec.2011.11.004>

Coccatto, A., Jehlick, J., Moens, L., Vandenabeele, P., 2015. Raman spectroscopy for the investigation of carbon-based black pigments. *J. Raman Spectrosc.* 46, 1003–1015. <https://doi.org/10.1002/jrs.4715>

Contreras, F., 2000. Proyecto Peñalosa. Análisis histórico de las comunidades de la Edad del Bronce del Piedemonte Meridional de Sierra Morena y Depresi3n Linares-Bailén, *Arqueología Monografías 10*. Conserjería de Cultura. Sevilla.

Contreras, F., Alarc3n, E., 2012. La cultura de Cogotas y las comunidades argáricas del Alto Guadalquivir: una perspectiva actual. In: Rodríguez Marcos, J.A., Fernández Manzano J. (Eds.), *Cogotas I. Una cultura de la Edad del Bronce en la Península Ibérica*. Universidad de Valladolid. Valladolid, pp. 165-185.

Contreras, F., Moreno, A., Arboledas, L., Alarc3n, E., Mora, A., Padilla, J.J., García, A., 2014. Un poblado de la Edad del Bronce que tiene mucho que decir, Peñalosa: últimas novedades en la acrópolis oriental. *Cuadernos de Prehistoria y Arqueología de la Universidad de Granada* 2, 347-390. <https://doi.org/10.30827/cpag.v24i0.4103>

Covertini, F., Querré, G., 1998. Apports des études céramologiques en laboratoire á la onnaissance du Campaniforme: résultat, bilans et perspectives. *Bulletin de la Société Préhistorique Francaise* 95, 333-341.

Douglas, T., Blitz, J., Burton, J., Ezzo, J.A. 1992. Diagenesis in Prehistoric Bone: Problems and Solutions, *J. Arch. Sci.* 19, 513-529. [https://doi.org/10.1016/0305-4403\(92\)90026-Y](https://doi.org/10.1016/0305-4403(92)90026-Y)

Elgamouz, A., Tijani, N. 2018. Dataset in the production of composite clay-zeolite membranes made from naturally occurring clay minerals. Data Brief 19, 2267-2278. <https://doi.org/10.1016/j.dib.2018.06.117>

Elgamouz, A., Tijani, N., Shehadi, I., Hasan, K., Al-Farooq, M., 2019. Characterization of the firing behaviour of an illite-kaolinite clay minerals and its potential use as membrane support. Heliyon 5 (8). <https://doi.org/10.1016/j.heliyon.2019.e02281>

Erdoğan, B., Dikmen, G., Alber, Ö., 2016. Investigation of the influence of heat treatment on the structural properties of illite-rich clay minerla usign FT-IR, si MAS NMGR, TG and DTA Methods. J. Sci. and Technology 17 (5), 823-829. <https://doi.org/10.18038/aubtda.279851>

Farooq. A., Muhhamad. A., Saman. A., Tabassum. S., Anwar. A., Rehman. I. 2013. Raman Spectroscopy of natural bone and synthetic apatites. Appied Spectroscopy Rev. 48(4), 329-355. <https://doi.org/10.1080/05704928.2012.721107>

Flude, S., Haschke, M., Storey, M. 2017. Application of benchtop micro-XRF to geological materials. *Mineral Mag.* 81, 923–948. <https://doi.org/10.1180/minmag.2016.080.150>

Freire, F., Acevedo, V., Halac, E.B., Polla, G., López, M., Reinoso, M., 2015. X-ray diffraction and Raman spectroscopy study of white decorations on tricolored ceramics from Northwestern Argentina. Spectrochim. Acta A Mol. Biomol. Spectrosc. 157, 182-185. <https://doi.org/10.1016/j.saa.2015.12.030>

Frost, R.L., Mendelovici, E., 2006. Modification of fibrous silicates surface with organic derivates: an infrared spectroscopic study. J. of Colloid and Interface Sci. 294, 47-52. <https://doi.org/10.1016/j.jcis.2005.07.014>

García González, D., Lozano, J.A., Carrión, F., López, C. F., 2010. Aprovechamiento de georrecursos en la cuenca alta del Río Rumblar (Jaén) en el II milenio a.C., in: Domínguez, S., Ramos, J., Gutiérrez, J.M., Pérez, M. (eds.), *Minerales y Rocas En Las Sociedades De La Prehistoria*. Grupo HUM-440, Universidad De Cádiz. Cádiz, pp. 321-330.

Garskaite, E., Gross, K. Yang, S.W, Chung-Kuang, T., 2013. Effect of processing conditions on the crystallinity and structure of carbonated calcium hydroxyapatite (CHAp). CrystEngComm 16 (19), 3950-3959. <https://doi.org/10.1039/C4CE00119B>.

Gherdán, K., Biró, K.T., Szakmany, G.Y., Tóth, M., SólyMos, K.G., 2003. Analysis of incrustrated pottery from Vörs, southwest Hungary. In: Prudêncio, I.M., Dias, M.I., Waerenborgh, J.C. (Eds.), *Understanding people throught their pottery*. Proceedings of the 7th European Meeting on ANcient Ceramics. *Trabalhos de Arqueologia* 42, 103-108.

Giustetto, G., Berruto, G., Diana, E., Costa, E., 2013. Decorated prehistoric pottery from Castello di Annone (Piedmont, Italy): archaeometric study and pilot comparison

with coeval analogous finds. *J. Arch. Sci.* 40, 4249-4263.
<http://dx.doi.org/10.1016/j.jas.2013.06.012>

Goldberg, M.A., Porsenko, P.V., Smirnob, V.V., Antonova, O.S., Smirnov S.V. Konovalov, A.A., Vorckachev, K.G., Kudryavtsev, E.A., Barinov, S.M., Komlev, V.S. 2020. The enhancement of hydroxyapatite thermal stability by Al doping. *J Mater Res Techolol* 9 (1): 76-88. <https://doi.org/10.1016/j.jmrt.2019.10.032>

González, A., Barroso, R., 1996-2003. El papel de las cazoletas y los cruciformes en la delimitación del espacio. Grabados y materiales del yacimiento de San Cristóbal (Valdemorales-Zarza de Montánchez, Cáceres). *Norba. Revista de Historia* 16, 75-121.

González-Tablas, F.J., 1984-85. Protocogotas o el bronce medio de la Meseta: La Gravera de 'Puente Viejo' (Ávila). *Zephyrus XXXVII-XXXVIII*, 267-276.

Gummesson, S., Molin, F., Sjöström, A., 2019. The spatial organization of bone crafting during the Middle and Late Mesolithic at Ringsjöholm and Strandvägen in Sweden. *J. of Field Archaeol.* 44, 165-179.
<https://doi.org/10.1080/00934690.2019.1580093>

Harrison R. J., 1995. Bronze Age Expansion 1750-1250 BC: The Cogotas I Phase in the Middle Ebro Valley. *Veleia* 12, 62-67.

Herliansyah, M.K., Hamdi, M., Ide-Ektessabi, A., Wildan, M.W. Toque, J.A., 2009. The influence of sintering temperature on the properties of compacted bovine hydroxyapatite. *Mater. Sci. and Eng. C* 29, 1674-1680,
<https://doi.org/10.1016/j.msec.2009.01.007>

Holck, P., 2005. Cremated bones. Anatomical Institute. University of Oslo, Oslo, pp. 113-119.

Hüls, CM, Erlenkeuser, H, Nadeau, M-J, Grootes, P.M, Andersen, N., 2010. Experimental study on the origin of cremated bone apatite carbon. *Radiocarbon* 52 (2-3), 587-99. <https://doi.org/10.1017/S0033822200045628>

IGME, 1976. Mapa geológico de España a escala 1/50.000. HOJA 884, Instituto Geominero de España. Madrid.

IGME, 2005. Caolín y caolinitas, Instituto Geominero de España. Madrid.

Jones, R., Towers, R., Card, N., Odling, N., 2019. Analysis of coloured Grooved Ware from sherds from the Ness of Brodgar, Orkney. *J. Arch. Sci. Rep.* 28, 102014.
<https://doi.org/10.1016/j.jasrep.2019.102014>

Kierdorf, U., Stoffels, D., Kierdorf, H., 2014. Element Concentrations and Element Ratios in Antler and Pedicle Bone of Yearling Red Deer (*Cervus elaphus*) Stags-a Quantitative X-ray Fluorescence Study. *Biological Trace Element Res.* 162, 124-133.
<https://doi.org/10.1007/s12011-014-0154-x>

Kos, K., Posilovic, H., Durman, A., Ristic, M., Krehula, S., 2015. White incrustation produced from deer antler phosphate on prehistoric ceramics from Produnavlje. *Archaeometry* 57, 636-652. <https://doi.org/10.1111/arc.12108>

Lambrecht, G., Mallol, C., 2020. Autofluorescence of experimentally heated bone: Potential archaeological applications and relevance for estimating degree of burning. *J. Arch. Sci. Rep.* 31. <https://doi.org/10.1016/j.jasrep.2020.102333>

Lantes-Suárez, O., Prieto-Martínez, M.A.P., Martínez Cortizas, A., 2010. Caracterización de pastas blancas incrustadas en decoraciones de campaniformes gallegos. Indagando sobre su procedencia. In: Saiz, M.E., López, R.L., Cano Díaz-Tendero, M.A.N., Calvo, J.C. (Eds.), VIII Congreso Ibérico de Arqueometría. ACTAS. Seminario de Arqueología y Etnología Turolense. Teruel. pp. 87-99.

Lebon, M., Reiche, I., Fröhlich, F., Bahain, J.J., 2008. Characterization of archaeological burnt bones: contribution of a new analytical protocol based on derivate FTIR spectroscopy and curve fitting of the $\nu^1 \nu^3$ PO₄ domain. *Anal. Bioanal. Chem.* 392, 1479-1488. <https://doi.org/10.1007/s00216-008-2469-y>

Lim, K.T., Kim, J.W., Kim, J., Chung, J.H., 2014. Development and Evaluation of Natural Hydroxyapatite Ceramics Produced by the Heat Treatment of Pig Bones. *J. Biosystems Engineering* 39 (3), 227-234. <https://doi.org/10.5307/JBE.2014.39.3.227>

López Padilla, J.A., Barciela, V., García Atienzar, G., Hernández, M.S., 2019. Deer antler objects production during Bronze Age in southeast of the Iberian peninsula. Cabezo Redondo (Villena, Alicante, Spain). *Cuadernos de Prehistoria y Arqueología de la Universidad de Granada* 29, 171-186. <https://doi.org/10.30827/cpag.v29i0.9771>

Mamede, A., Gonçalves, D., Marques, M.P., Batista, L., 2017. Burned bone tells their own stories: A review of methodological approaches to assess heat-induced diagenesis. *Applied Spectroscopy Review*, 1-33. <https://doi.org/10.1080/05704928.2017.1400442>

Marques, M.P.M, Mamede, A.P., Vassalo, A.R., Makhoul, C., Cunha E., Gonçalves, D., Parker, S.F., Batista de Carvalho, L.A.E., 2018. Heat-induced bone diagenesis probed by vibrational spectroscopy. *Sci. Rep.* 8, 15935. <https://doi.org/10.1038/s41598-018-34376-w>.

Martín-Gil, J.; Martín-Gil, F.J., 2009. Caracterización de una pasta blanca de relleno en las decoraciones de la Edad del Bronce de “El Pelambre”. In González Fernández, M.L. (Ed.), *El Pelambre* (Villaornate, León). *El horizonte Cogotas I de la Edad del Bronce y el período tardoantiguo en el Valle Medio del Esla*. Grupo Tragsa, S.L., pp. 187-189.

Middleton, A.P., Edwards, H.G.M., Middleton, P.S., Ambers, J., 2005. Identification of anatase in archaeological materials by Raman spectroscopy: implications and interpretation. *J. Raman Spectroscopy* 36, 984-987. <https://doi.org/10.1002/jrs.1394>

Munro, L.E., Longstaffe, F.J., White, C.D., 2007. Burning and boiling of modern deer bone: Effects on crystallinity and oxygen isotope composition of bioapatite phosphate. *Paleogeography, Paleoclimatology, Palaeoecology* 249, 90-102. <https://doi.org/10.1016/j.palaeo.2007.01.011>

Odriozola, C.P., Hurtado, V.M., 2005. Tecnología y producción de decoraciones cerámicas campaniformes con relleno de hueso en la cuenca media del Guadiana, In: VI Congreso Ibérico de Arqueometría. Girona: 71-19.

Odriozola, C.P., Hurtado, V.M., 2007. The manufacturing process of 3rd millennium BC bone based incrustrated pottery decoration from the Middle Guadiana river basin (Badajoz, Spain). *J. Arch. Sci.* 34, 1794-1803. <https://doi.org/10.1016/j.jas.2006.12.021>

Odriozola, C., Martínez-Blanes, J. M., 2007. Estimate of firing temperatures through bone-based chalcolithic decorated pottery. *J. Thermal Anal. Calorimetry* 87 (1), 135–141. <https://doi.org/10.1007/s10973-006-7833-6>

Odriozola, C.P., Hurtado, V. M., Guerra, E., Cruz-Auñón, R., Delibes, G., 2012. Los rellenos de pasta blanca en cerámicas campaniformes y su utilización en la definición de límites sociales. In: Isabel Dias, M., Cardoso, J.L. (Eds.), *Actas do IX Congresso Ibérico de Arqueometria*. Lisboa. Câmara municipal de Oeiras. Lisboa, pp. 143-154.

Odriozola, C., 2018. Informe: relleno de pasta blanca de la cerámica de casas novas. In: Gonçalves, V., Sousa, A.C. (Eds.), *Casas Novas, numa curva do Sorraia (no 6º milénio a.n.e. e a seguir)*. Centro de Arqueologia da Universidade de Lisboa. Lisboa.

Parkinson, W.A., Peacock, E., Palmer, R.A., Xia, Y., Carlock, B., Gyucha, A., Yerkes, R.W., Galaty, M.L., 2010. Elemental analysis of ceramic incrustation indicates long-term cultural continuity in the prehistoric carpathian basin. *Archaeology, Ethnology and Anthropology of Eurasia* 38 (2), 64-70. <https://doi.org/10.1016/j.aeae.2010.08.009>

Perišić, N., Marić-Stojanović, M., Andrić, V., Mioč, U.B., Damjanović, L., 2016. Physicochemical characterisation of pottery from the Vinča culture, Serbia, regarding the firing temperature and decoration techniques. *J. Serbian Chem. Soc.* 81 (12), 1415-1426.

Pirovska, A., Antonova, K., Malcheva, G., Tankova, V., Blagoev, K., 2020. Nature and physicochemical features of the incrustrated white decoration on pottery from two sites in Bulgaria, dated to the chalcolithic period (IV mil BC). *J. Arch. Sci. Reports.* 29. <https://doi.org/10.1016/j.jasrep.2019.102142>

Pucéat, E., Reynard, B., Lecuyer, C., 2004. Can crystallinity be used to determine the degree of chemical alteration of biogenic apatites?. *Chem. Geology* 205, 83–97. <https://doi.org/10.1016/j.chemgeo.2003.12.014>

Roberts, S., Sofaer, J., Kiss V., 2008. Characterization and textural analysis of Middle Bronze Age Transdanubian inlaid wares of the Encrusted Pottery Culture, Hungary: a preliminary study. *J. Arch. Sci.* 35, 322-330. <https://doi.org/10.1016/j.jas.2007.03.013>

Rousseau, R. M. (2004). Some considerations on how to solve the Sherman equation in practice. *Spectrochim. Acta B.* 59, 1491–1502. <https://doi.org/10.1016/j.sab.2004.06.002>

Saikia, B., Parthasarathy, G., 2010. Fourier Transform Infrared Spectroscopic characterization of kaolinite from Assam and Meghalaya, Northeastern India. *J. Modern Phys.* 1, 206-210. <http://doi.org/10.4236/jmp.2010.14031>

Sánchez, A., Tuñón, J.A., Parras, D.J., Montejo, M., Lechuga, M.A., Ceprián, B., Soto, M., Luque A., 2019. MRS, EDXRF y GC-MS analysis for research on the ritual and funerary areas of Cerro de los Vientos (Baeza, Jaén, Spain). *Native and Eastern Mediterranean Influences. J. Arch. Sci. Rep.* 28, 1-14. <https://doi.org/10.1016/j.jasrep.2019.102026>

Sanz, J. L., Morales, A., 2000. Los restos faunísticos. In: Contreras, F. (Ed.), *Proyecto Peñalosa. Análisis histórico de las comunidades de la Edad del Bronce del Piedemonte Meridional de Sierra Morena y Depresión Linares-Bailén*, Arqueología Monografías 10. Conserjería de Cultura. Sevilla.

Schibler, J., 2001. Experimental production of Neolithic bone and antler tools. In: Choyke, A.M., Bartosiewicz, L. (Eds), *Crafting bone: Skeletal technologies through time and space*. BAR International Series. Archaeopress 2011. Oxford, pp. 49-60.

Shoval, S., Yadin, E., Panczer, G., 2011. Analysis of thermal phases in calcareous Iron Age pottery using FT-IR and Raman spectroscopy. *J. Therm. Anal. Calorim.* 104, 515–525. <https://doi.org/10.1007/s10973-011-1518-5>

Schubart. H., Ulreich, H., 1991. Die Funde der Südostspanischen Bronzezeit aus der smmlung Siret. *Madrider Beiträge*, 17. Madrid.

Sofaer, J., Roberts, S., 2016. Technical innovation and practice in Eneolithic and Bronze Age encrusted ceramic in the Carpathian Basin, Middle and Lower Danube. *Archaologische Korrespondenzblatt* 46 (4), 479-496.

Starkovich, B.M., Hodgins, G.W.L., Voyatzis, M.E., Gilman, D., 2013. Dating gods: Radiocarbon dates from the sanctuary of Zeus on MT Lykaion (Arcadia, Greece). In: Jull, A.J.T., Hatté, C., (Eds), *Proceedings of the 21st International Radiocarbon Conference* 55, 501-513.

Sziki, G.A., Biró, K.T., Uzonyi, I., Dobos, E., Kiss, A.Z., 2003. Investigation of incusted pottery found in the territory of Hungary by micro-PIXE method. *Nucl. Instrum. Methods in Phys. Res. Sect. B: Beam Interactions with Mater. and Atoms* 210, 478-482. [https://doi.org/10.1016/S0168-583X\(03\)01086-3](https://doi.org/10.1016/S0168-583X(03)01086-3)

Thomas, D.B., MacGoverin, C.M., Fordyce, R.E., Frew, R.D., 2011. Raman spectroscopy of fossil bioapatite. A proxy for diagenetic alteration of the oxygen isotope composition. *Palaeography, Palaeoclimatology, Paleoecology* 310, 62-70. <https://doi.org/10.1016/j.palaeo.2011.06.016>

Thompson, T.J.U., Islam, M., Bonniere, M., 2013. A new statistical approach for determining the crystallinity of heat-altered bone mineral from FTIR spectra. *J. Arch. Sci.* 40, 416-422. <https://doi.org/10.1016/j.jas.2012.07.008>

Tuñón, J., Sánchez, A., Parras, D., Vandenabeele, P., Montejo, M., 2016. Micro-Raman Spectroscopy on the Iberian archaeological materials. *J. Raman Spectroscopy* 47, 1514-1521. <https://doi.org/10.1002/jrs.4934>

Tuñón, J., Sánchez, A., Parras, D.J., Amate, P., Montejo, M., Ceprián, B., 2020. The colours of Rome in the walls of Cástulo (Linares, Spain). *Sci. Rep.* 10 (1),12739. <https://doi.org/10.1038/s41598-020-69334-y>

Van Strydock, M., Boudin, M., De Mulder, G., 2010. The carbon origin of structural carbonate in bone apatite of cremated bones. *Radiocarbon* 52 (2-3), 578-86. <https://doi.org/10.1017/S0033822200045616>

Vico, L., 2021. La cerámica argárica de Peñalosa (Baños de la Encina, Jaén). Estudio tipológico, tecnológico y decorativo de las vasijas de contextos domésticos y funerarios. Unpublished PhD thesis. University of Granada. Spain.

Všianský, D., Kolář, J., Petřík, J., 2014. Continuity and changes of manufacturing traditions of Bell Beaker and Bronze Age encrusted pottery in the Morava river catchment (Czech Republic). *J. Arch. Sci.* 49, 414-422. <http://dx.doi.org/10.1016/j.jas.2014.05.028>

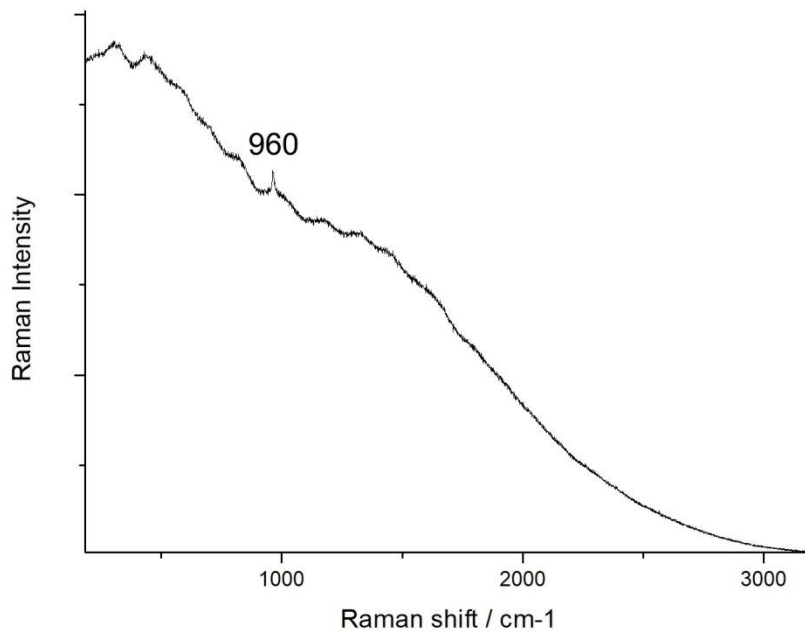
Walker, P.L., Miller, K., Richman, R., 2008. Time, temperature and oxygen availability: an experimental study of the effects of environmental conditions on the color and organic content of cremated bone. In: Schmidt, C.W., Symes, S. (Eds.), *The analysis of burned human remains*, Elsevier Press, Amsterdam, pp. 129-135. <https://doi.org/10.1016/B978-012372510-3.50009-5>

Wright, L.E., Schwarcz, H.P., 1996. Infrared and isotopic evidence for diagenesis of bone apatite at Dos Pilas, Guatemala: palaeodietary implications. *J. Arch. Sci.* 23, 933-944. <https://doi.org/10.1006/jasc.1996.0087>

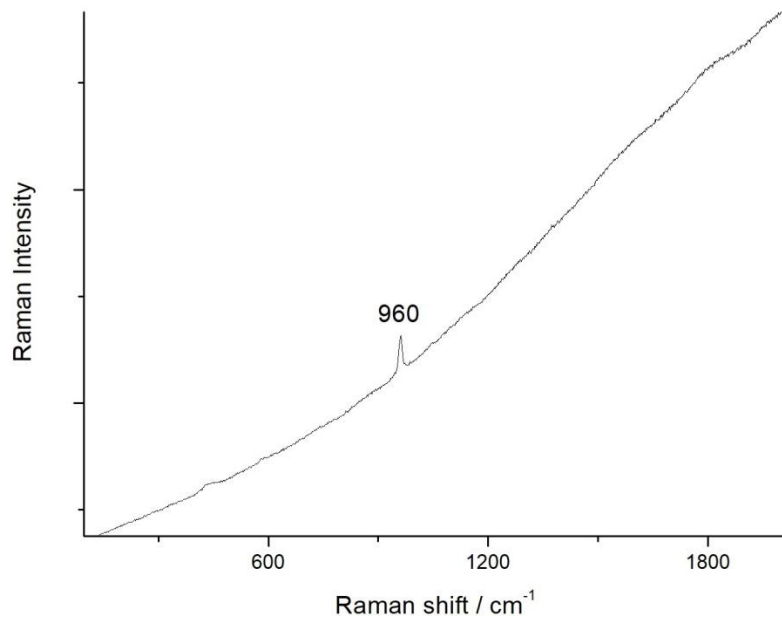
Zastawny, A., Rauba-Bukowska, A., Trąbska, J., Trybalska, B., 2012. Results of the microscopic Analyses of Vessels from Assemblages of the Modlnica Type (with Furchenstichkeramik) from Site 5 in Modlnica, Kraków District, Poland. *Interdisciplinaria Archaeologica* III (2), 257-277. [10.24916/iansa.2012.2.8](https://doi.org/10.24916/iansa.2012.2.8)

Zviagina, B.B., Drits, V.A., Dorzhieva, O.V., 2020. Distinguishing features and identification criteria for K-Dioctahedral 1M Micas (Illite-Aluminoceladonite and Illite-Glaucanite-Celadonite series) from Middle-Infrared spectroscopy data. *Minerals* 10, 1-29. <https://doi.org/10.3390/min10020153>

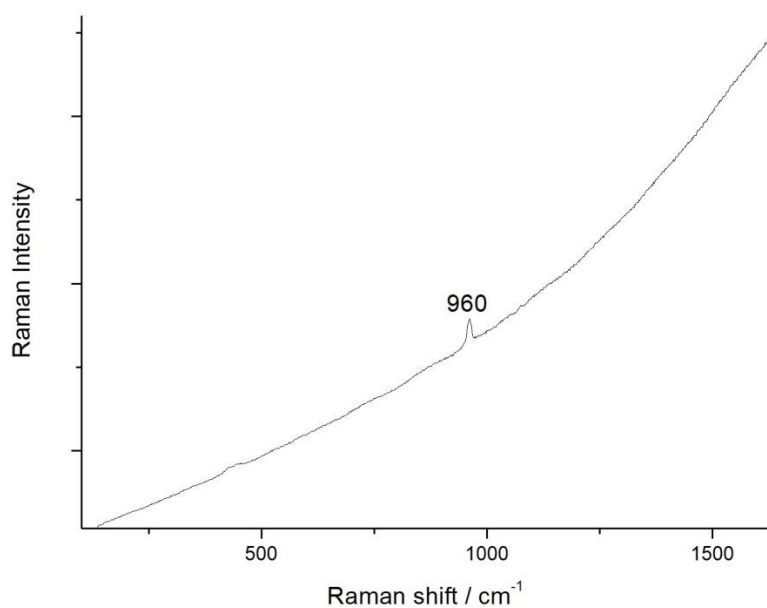
Supplementary data



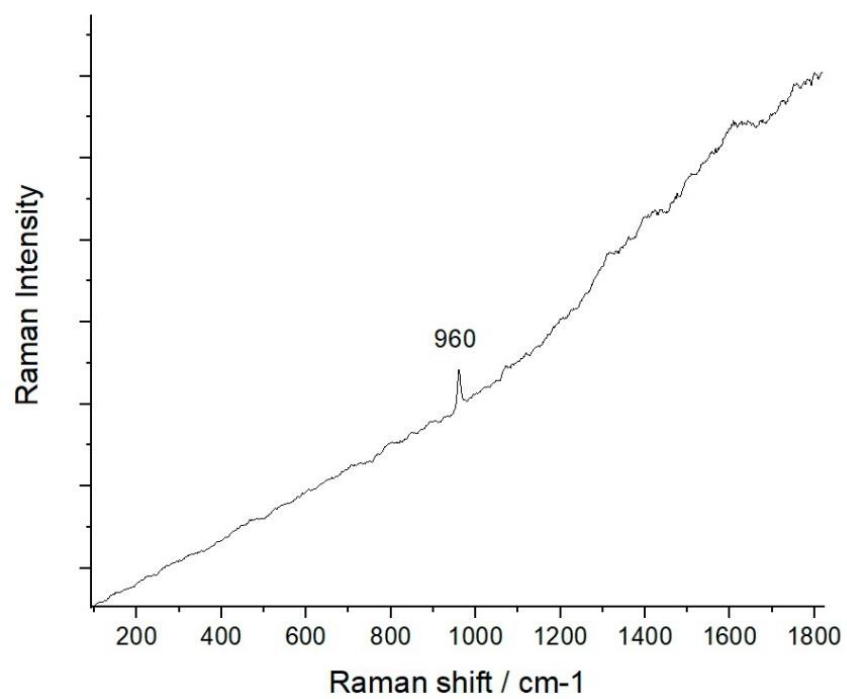
MRS results. Sample BE-28497-2. Experimental conditions: 50x objective, 50 accumulations of 10 s, 785 nm diode laser, 2.5 mW.



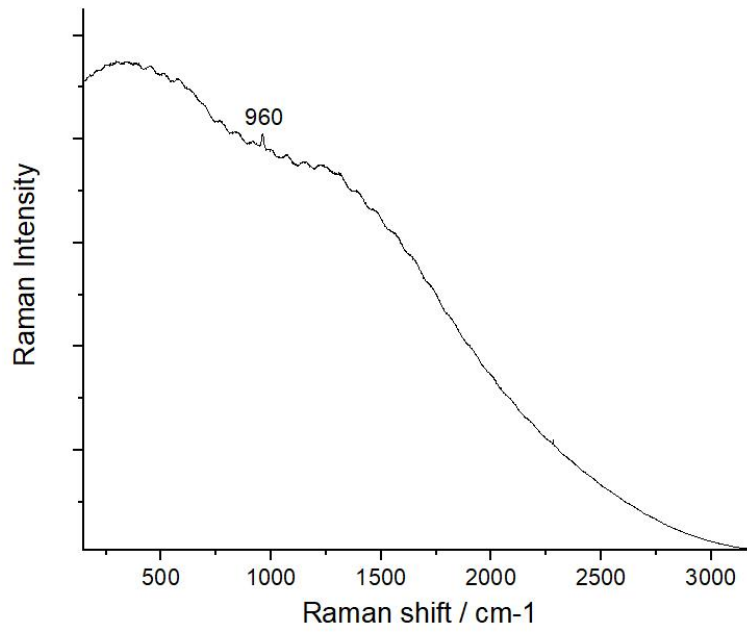
MRS results. Sample BE-28508-1. Experimental conditions: 50x objective, 50 accumulations of 10 s, 532 nm argon ion laser, 2.5 mW.



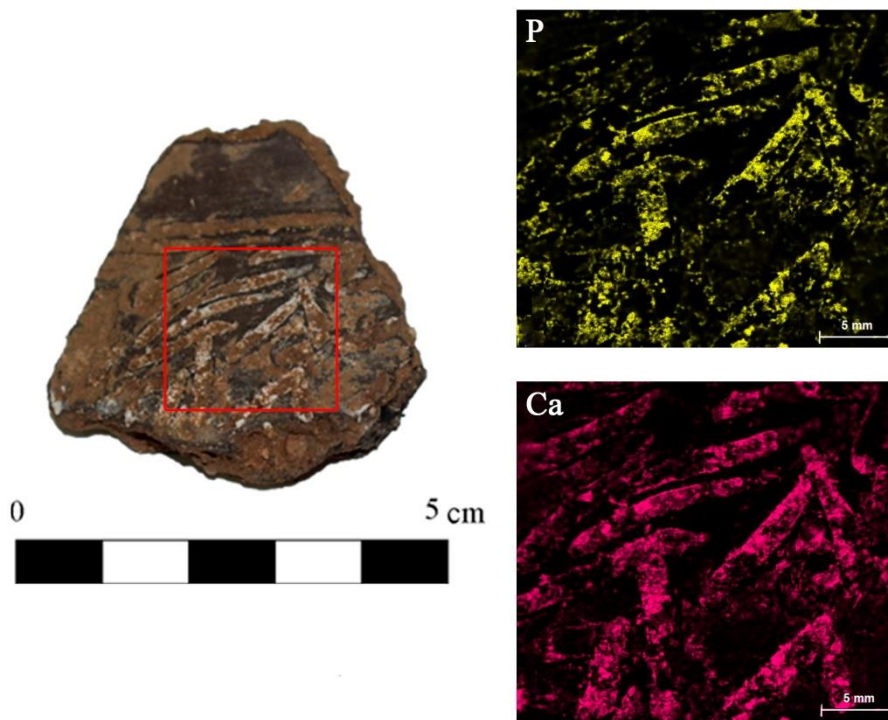
MRS results. Sample BE-28570. Experimental conditions: 50x objective, 50 accumulations of 10 s, 532 nm argon ion laser, 2.5 mW.



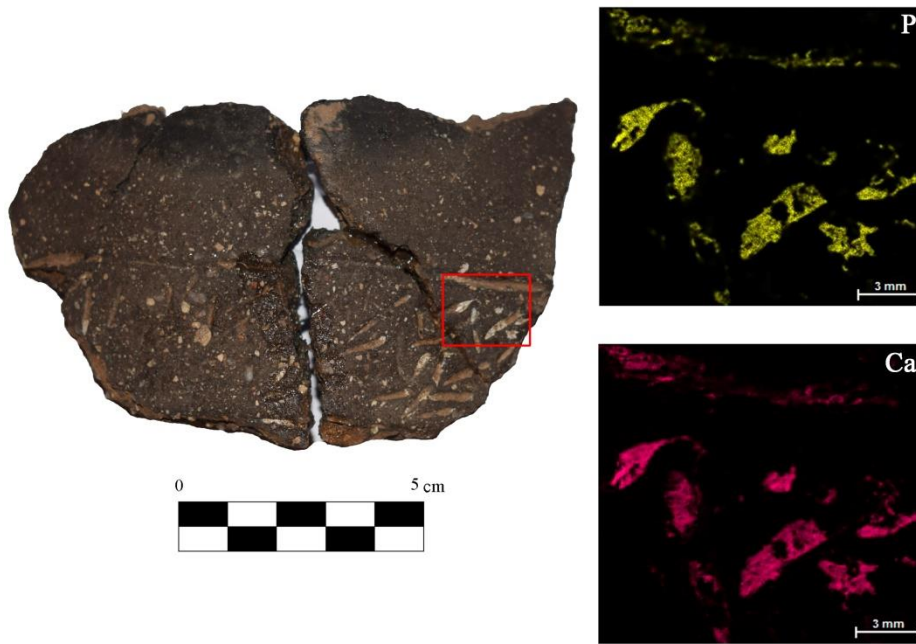
MRS results. Sample BE-25405-2. Experimental conditions: 50x objective, 50 accumulations of 10 s, 532 nm argon ion laser, 2.5 mW.



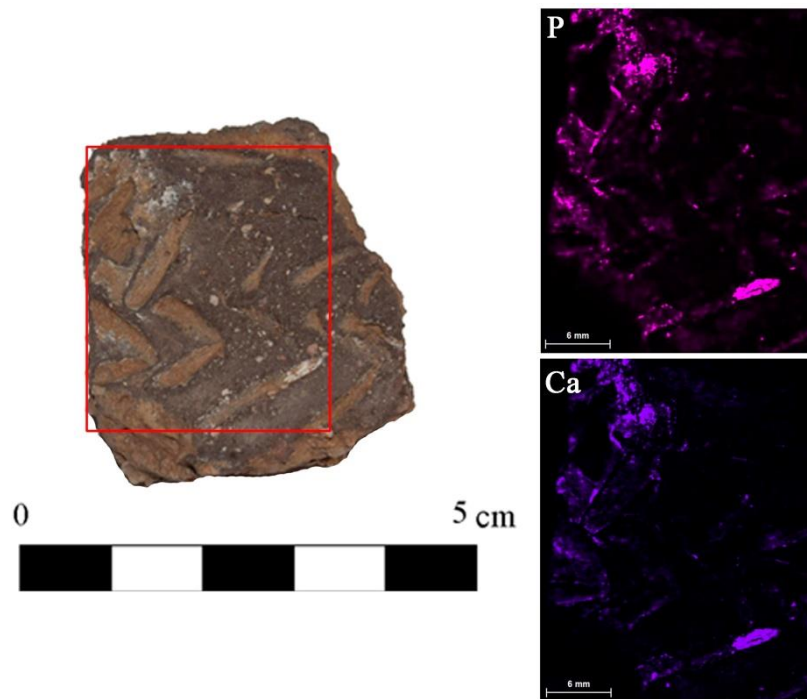
MRS results. Sample BE-25308. Experimental conditions: 50x objective, 50 accumulations of 10 s, 785 nm diode laser, 2.5 mW.



μ EDXRF mapping analysis of Ca and P in ceramic fragment BE-28497-2.



μ EDXRF mapping analysis of Ca and P in ceramic fragment BE-28508.



μ EDXRF mapping analysis of Ca and P in ceramic fragment BE-28570.